THERMODYNAMIC AND STRUCTURAL PROPERTIES OF HCP METALS AND BINARY ALLOYS

G. S. AGUNBIADE[1], F. MATTHEW-OJELABI[1], T. H. AKANDE[1],
A. I. OGUNDARE[2], O. O. AWE[3]

[1] Department of Physics, Ekiti State University, Ado Ekiti, Nigeria
E-mail: gbenga.agunbiade@eksu.edu.ng; fadeke.ojelabi@eksu.edu.ng;
taiwo.akande@eksu.edu.ng
[2] Department of Physics, Federal University of Agriculture, Abeokuta, Nigeria
E-mail: ogundare_adewale@yahoo.com.
[3] Department of Basic Sciences, Physics Electronics Unit, Babcock University, Nigeria
E-mail: aweo@babcock.edu.ng

Abstract. The *modified embedded-atom method*, MEAM for hcp Mg & Ti metals and alloys have been designed. The monovacancy formation, migration and activation energies in the hcp out plane were computed and reasonably agree with available data from experiments. The divacancy formation and binding energies of the first nearest-neighbour were reported. The computed value for the binding energy is positive, an indication of stability. The five independent elastic constants in hcp metals were determined and they all correlate with the experimental values. Finally, the enthalpy of solution for $Mg^H Ti^G$ and $Mg^G Ti^H$ binary alloys were considered. The values are positive but data from experiment are unavailable. For a better comparism, data from experiment are seriously needed.

Key words: Modified embedded-atom method, hcp metals, enthalpy of solution.

1. INTRODUCTION

The studying and understanding the structures and properties of any material for optimal technological applications are some of the keys to major technological advancement. Magnesium for instance, is an innocuous metal having the lowest density among other metals. As a result of its low density and affordability, it is commonly used for light alloys [1]. In the same vain, its fracture toughness coupled with its good mechanical strength makes it a great metal for lightweight material for load bearing applications [2, 3]. Magnesium and its alloys are also unique and excellent materials for aircraft and automobile industries. Due to its low Young modulus, it serves as a suitable material for biomedical orthopedic implants [4] but the major limitation in the applications of Mg is its low corrosion resistance.

Titanium is a non-magnetic and high corrosive resistance metal. It is highly used for aircraft structures, drilling equipment, gas turbines and biomedical

implants [5]. Alloying Mg with Ti will actually improve the low corrosion resistance found in Mg and to achieve this, a detailed atomistic simulation of these materials (Mg and Ti) must be investigated for maximum utilization. Previous techniques like the first principle potentials cannot adequately describe the interactions between these elements. So, in studying these materials, one of the most popular, accurate and effective multi-body potentials called embedded atom method, EAM that uses higher orders term with local density dependence will be employed.

The embedded atom method, EAM was developed over three decades ago [6]. The EAM potentials were constructed for face centred-cubic (fcc) metals and alloys [7–9], in a like manner, the EAM model was formulated for body centred-cubic (bcc) metals without considering their alloys [10]. Their generated results are good with available data from the experiments. With the EAM, an n-body potential for Zr-Nb alloy was presented by Lin and coworkers [11], the thermodynamic properties of Zr and Nb metals were computed. By considering the direction of the bonding, a modification part was added to original EAM [12] it was named the modified embedded-atom method, MEAM. This MEAM model was extended to bcc transition metals to calculate the thermodynamic properties of bcc metals [13]. Zhang and Quyang [14] applied the EAM to study the properties of hexagonal closed-package (hcp) binary alloys and concluded that the formation energy of Co-Y alloy is weak. Recently, we [15–17] applied the EAM to study various properties of the bcc and fcc metals and alloys. The EAM unlike previous potentials such as the LJ potential takes into consideration the effect of multi-body interactions of atoms and thereby accurately predicts the elastic properties better than the pair potentials. Up till date, several studies have been conducted for many bcc and fcc metals and alloys with limited work on the hcp metals and alloys.

The reason for our present article is to study the thermodynamic and structural properties of hcp Mg & Ti metals and alloys used for many technological tools and equipment by applying a robust and versatile multi-body interatomic potential known as the MEAM. We shall in details give the computational procedures, simulation method and also list the input physical quantities needed in fitting the curve of MEAM potential in section 2. We shall report and also discuss our computed results for these metals and alloys in section 3. Our section 4 will finally summarize and conclude the work.

2. SIMULATION METHOD

In this section, we shall in details give the simulation method and computational procedures for investigating the hcp Mg & Ti metals and alloys. The input physical quantities needed in fitting the curve of MEAM potential shall be presented as well.

2.1. THE EAM AND MEAM MODELS

In EAM, the sum of two terms gives the total energy which is written as:

$$E_t = F(\rho_i) + \frac{1}{2}\sum_{i \neq j}\phi(r_{ij}) \tag{1}$$

$F(\rho_i)$ and $\phi(r_{ij})$ are respectively the embedding and the two-body (pair) potential energies of a system of an atom.

To adequately describe the system of hcp metals and alloys, three terms will be required. A modification $M(P_i)$ term must be introduced to the initial energy of the EAM in (1).

Now, in MEAM, the total energy will be constructed as:

$$E_t = F(\rho_i) + \frac{1}{2}\sum_{i \neq j}\phi(r_{ij}) + M(P_i) \tag{2}$$

The first, second and third terms in (2) will explicitly be determined.

The electron density ρ_i and P_i as expressed by [10] is given as:

$$\rho_i = \sum_{i \neq j} f(r_{ij}) \tag{3}$$

and

$$P_i = \sum_{i \neq j} f^2(r_{ij}) \tag{4}$$

While $f(r_{ij})$ is the atomic electron density, r_{ij} remains the separation between atoms i and j.

The first term in (2) is an embedding function $F(\rho_i)$ which takes the form:

$$F(\rho_i) = -F_0\left[1 - n\ln\left(\frac{\rho_i}{\rho_e}\right)\right]\left(\frac{\rho_i}{\rho_e}\right)^n \tag{5}$$

$$F_o = E_c - E_{1f} \tag{6}$$

ρ_e and F_o are the electron density and the embedding function evaluated at equilibrium. E_{1f} and E_c are the mono-vacancy formation and cohesive energies respectively.

The second term is a two-body potential $\phi(r_{ij})$ and is also given as:

$$\phi(r_{ij}) = K_a + K_b \left(\frac{r_{ij}}{r_{1e}}\right)^2 + K_c \left(\frac{r_{ij}}{r_{1e}}\right)^4 + K_d \left(\frac{r_{ij}}{r_{1e}}\right)^{-12} \tag{7}$$

$$\left(\text{for } r_{ij} \leq r_{2e}\right)$$

r_{1e} and r_{2e} are respectively at equilibrium the first- and second-nearest neighbour distances.

The third term is a modified term $M(P_i)$ that will be obtained as:

$$M(P_i) = \alpha \left(\frac{P_i}{P_e} - 1\right)^2 \ell \ x \ \rho\left[-\left(\frac{P_i}{P_e} - 1\right)^2\right] \tag{8}$$

The present model parameters can all be evaluated using (9–12).
n in (5) is parameterization and is obtained as:

$$n = \sqrt{\frac{\Omega\chi(C_{11} + 2C_{12})}{216 E_{1f} C_{44}}} \tag{9}$$

$$\chi = C_{11} - C_{12} \tag{10a}$$

The atomic volume, Ω for our present work is chosen as:

$$\Omega = \frac{a_0^2 c\sqrt{3}}{4} \tag{10b}$$

where, a_o, c, C_{11}, C_{12} & C_{44} are the lattice and elastic constants of the hcp metals.
The model parameters K_a, K_b, K_c and K_d in (7) is obtained as

$$K_a = -\frac{E_{1f}}{9} - \frac{\Omega(8470\chi - 17437 C_{44})}{42840} \tag{11a}$$

$$K_b = \frac{\Omega(2250\chi - 5067 C_{44})}{9520} \tag{11b}$$

$$K_c = \frac{-\Omega(65\chi - 161 C_{44})}{1887200} \tag{11c}$$

$$K_d = \frac{8\Omega(10\chi - 13 C_{44})}{5355} \tag{11d}$$

$$\alpha = \frac{\Omega\left(C_{12} - C_{44}\right) - 4n^2 F_0}{32} \tag{12}$$

The atomic electron density between two atoms i and j is

$$f(r_{ij}) = f_e \left(\frac{r_{1e}}{r_{ij}}\right)^6 \tag{13a}$$

f_e is the atomic electron density evaluated at equilibrium and is given by

$$f_e = \left(\frac{E_c - E_{1f}}{\Omega}\right)^{3/5} \tag{13b}$$

2.2. ALLOY MODEL FOR HCP

The alloy model for the present work is a modification of [8] model designed for bcc metals. The atomic volume of each hcp metal is considered for both the host (solvent) and the guest (solute) atoms. The density of atom i at any site, is a linear addition of all other atoms' densities. With this, mixing rule for densities is of no need.

The cross potentials between the host (H) and guest (G) atoms using a mixing rule is presented as:

$$\phi^{HG} = \frac{1}{2}\left[\frac{\Omega_G f_G(r)}{\Omega_H f_H(r)}\phi^{HH}(r) + \frac{\Omega_H f_H(r)}{\Omega_G f_G(r)}\phi^{GG}(r)\right] \tag{14}$$

While Ω_H and Ω_G are respectively the atomic volume of the host and the guest atoms, f_H and f_G are the atomic electron densities of the host and the guest atoms.

To compute the enthalpy of solution (unrelaxed) of hcp the following steps will be examined:

(i) an energy is needed to remove the host (solvent) atom

$$\Delta H_A = -F^H(\rho^H) - \sum_{i \neq 1}\phi^{HH}(r_e^H) \tag{15}$$

(ii) another energy is required to add the guest (solute) atom

$$\Delta H_B = F^G(\rho^H) + \sum_{i \neq 1}\phi^{GH}(r_e^H) \tag{16}$$

(iii) energy to adjust neighbouring atoms

$$\Delta H_C = -\sum_{i \neq 1} F_i^H(\rho^H) + \sum_{i \neq 1} F_i^H(\rho_e^H + \Delta\rho) \tag{17}$$

$$\Delta\rho = -f^H(r_e^H) + f^G(r_e^H)$$

ρ_e^H and r_e^H are respectively the equilibrium electron density and the equilibrium-nearest neighbour separation of the host atom.

(iv) finally, an energy to get the cohesion energy adjusted

$$\Delta H_D = -E_c^H + E_c^G \tag{18}$$

Therefore, the enthalpy of solution ΔH (unrelaxed) is the summation (15–18) of all these energy terms

$$\Delta H = \Delta H_A + \Delta H_B + \Delta H_C + \Delta H_D \tag{19}$$

To compute the relaxed enthalpy of solution another term is needed to be added to (19). The relaxation term was presented by [18] and was used previously used for bcc alloys by [16].

This term [18] is given as:

$$E_R = -\left[1.167\left(\frac{\Omega_G}{\Omega_H} - 1\right)\right]^2 \tag{20}$$

The input physical quantities, lattice parameters, cohesive & vacancy-formation energies and elastic constants (C_{11}, C_{12}, C_{13}, C_{33}, C_{44}) needed in fitting the curve of the potential were taken from different literatures and are listed in Table 1.

Table 1

The input physical quantities for hcp Mg and Ti metals. The lattice constants, (a_0 and c) and the cohesive energy were taken from [19]. While the mono-vacancy energy for Mg and Ti was taken respectively from [20] and [22], the elastic constants were also taken from [21] and [23] respectively

Quantity	Mg	Ti
a_0 (Å)	3.21	2.95
c (Å)	5.21	4.68
E_c (eV)	1.53	4.846
E_{If} (eV)	0.58	1.41
C_{11} (eV/Å^3)	0.37	1.021
C_{12} (eV/Å^3)	0.16	0.576
C_{13} (eV/Å^3)	0.136	0.424
C_{33} (eV/Å^3)	0.384	1.156
C_{44} (eV/Å^3)	0.102	0.294

3. RESULTS AND DISCUSSION

All the eight model parameters needed in constructing a complete and useful MEAM model for the present work are listed in Table 2. These parameters are evaluated using the monovacancy and cohesive energies, lattice constants and five independent elastic constants of hcp metals listed in Table 1 and by applying equations (6–13). The pair potentials and the embedding functions for pure hcp Mg & Ti metals are shown in Fig. 1 and Fig. 2 respectively. The minimum of the pair potentials is distinctly observed and is close to the nearest-neighbour distance.

Table 2

The MEAM model parameters for the hcp Mg & Ti. While the parameters n and f_e are dimensionless, parameters F_0, α, K_a, K_b, K_c and K_d are in eV

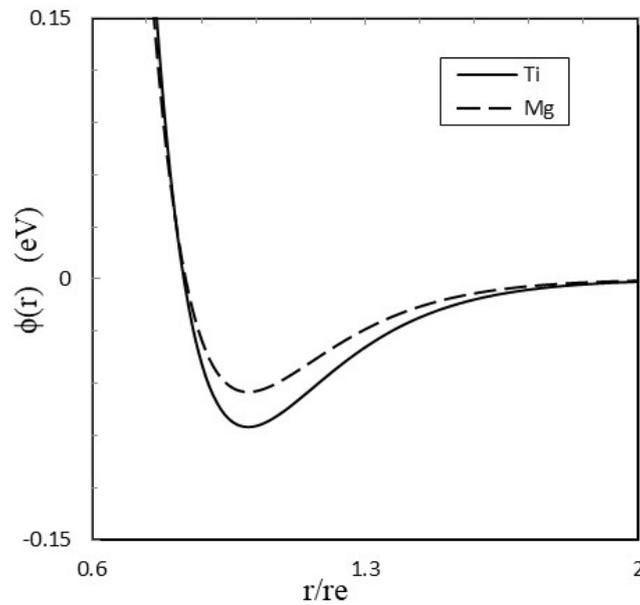| Metal	F_0	f_e	n	α	K_a	K_b	K_c	K_d
Mg	0.7600	0.1285	0.4514	0.0228	−0.0834	−0.1082	0.0632	0.0269
Ti	3.4460	0.3755	0.4364	0.0734	0.4021	−0.9048	0.3183	0.0165

Fig. 1 – The plot of the pair potential against the relative distance for Mg and Ti metals

With the present model, the vacancy formation and migration energies are determined, the sum of which is the activation energy is also computed. It is noted that the migration energy in hcp metals can either be an atom going out of the plane (out-plane) or coming in to the plane (in-plane) as a result of two different saddle points found in hcp. For this work, the migration and the activation energies for self-diffusion out-plane as shown in Table 3 are only reported because there is

little or no difference between these energies both in-plane and out-plane for the metals considered.
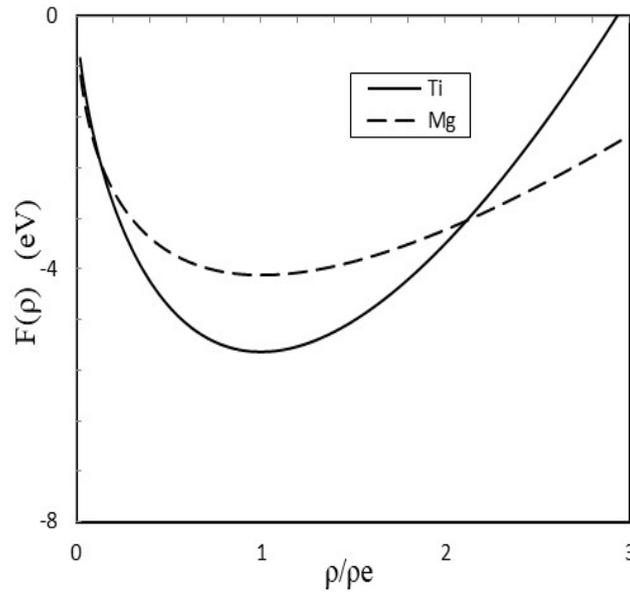

Fig. 2 – The plot of the embedding energy against relative density for Mg and Ti metals.

Table 3

The computed and experiment data for the monovacancy formation E_{1f},
migration $E_1 m$ and activation Q_{1v} energies of hcp Mg & Ti metals

Metal	E_{1f} (eV)		$E_1 m$ (eV)		Q_{1v} (eV)	
	Present work	Exp. [9]	Present work	Exp.	Present work	Exp.
Mg	0.63	0.58	0.42	0.39 [25]	1.05	1.38 [26]
Ti	1.46	1.41	0.65	0.67 [24]	2.11	2.16 [24]

The correlation between our computed results for these energies in Table 3 with the available data from experiment are reasonably good. There are no available experimental data for the $E_1 m$ and Q_{1v} of Ti so our computed results are only compared with results from [24] and are very close to each other.

Though there are limited works concerning divacancy in hcp metals, the divacancy formation and binding energies for the first nearest-neighbour are also considered. The computed values are reported in Table 4. The result of the computed binding energy is positive for both Mg and Ti which is an indication of stability. Hu and coworkers [27] calculated the divacancy formation and binding energies for hcp Mg, while Johnson [24] obtained these energies for Ti. Their calculated values are in better agreement with our computed values.

Table 4

The computed and experimental data for the divacancy formation E_{2f}, and binding energies
of hcp Mg & Ti metals

Metal	E_{2f} (eV)		*Binding energy* (eV)	
	Present work	Exp.	Present work	Exp.
Mg	1.165	1.10 [27]	0.095	0.08 [27]
Ti	2.73	2.76 [24]	0.19	0.22 [24]

Table 5

The elastic constants of hcp Mg and Ti metals. While the data from experiment for the elastic
constants of Mg are taken from [21], the data for Ti are taken [23]

Metal	C_{11} (eV/Å^3)		C_{12} (eV/Å^3)		C_{13} (eV/Å^3)		C_{33} (eV/Å^3)		C_{44} (eV/Å^3)	
	Present work	Exp.	Present work	Exp.	Present work	Exp.	Present work	Exp.	Present work	Exp.
Mg	0.359	0.370	0.161	0.160	0.139	0.136	0.378	0.384	0.105	0.102
Ti	1.035	1.021	0.561	0.576	0.440	0.424	1.140	1.156	0.301	0.294

Table 6

The computed heats of solution (unrelaxed and relaxed) for possible binary alloys of Mg and Ti.
While (H) denotes the host atom (solvent), G denotes guest atom (solute)

Alloy	ΔH (eV)	
	Unrelaxed	Relaxed
$Mg^H Ti^G$	0.18	0.15
$Ti^H Mg^G$	0.14	0.12

The elastic constants from which the bulk, young and shear moduli can be obtained were calculated and reported in Table 5. The computed values when compared with the data from experiment are also good. The enthalpy of solution (relaxed and unrelaxed) for Mg as host atom (Mg^H) & Ti as the guest (Ti^G) and *vice versa* were predicted as shown in Table 6. The cohesive energy and the lattice constant play a vital role in predicting the enthalpy of solution of alloys. When both the cohesive energy and the atomic size of the host atom (solvent) are either less or greater than that of the guest atom (solute), negative value of the enthalpy of solution is mostly predicted but zero when the cohesive and the lattice constant are almost the same for both the host and the guest atoms.

However, the predicted value of the enthalpy of solution is expected to be positive when the atomic size of the host atom is greater than the guest, and the cohesive energy of the host atom is less than its corresponding guest atom or *vice versa*. For our present work, the enthalpy of solution is positive for both $Mg^H Ti^G$ and $Mg^G Ti^H$. The experimental value for this alloy is seemly unavailable at present, so for better comparism, the data from experiment is highly needed.

4. CONCLUSIONS

The modified embedded-atom method, MEAM for hcp Mg & Ti metals and alloys have been designed. The potentials were fitted to elastic constants, lattice parameters, monovacancy formation and cohesive energies. All the eight model parameters needed in constructing a useful MEAM model for the present work were evaluated. The monovacancy formation, migration and activation energies in the hcp out plane are reasonably agree with available data from experiments. The divacancy formation and binding energies of the first nearest-neighbour were reported. Finally, the enthalpy of solution (unrelaxed and relaxed) for $Mg^H Ti^G$ and $Mg^G Ti^H$ binary alloys were considered. The values are positive but there are no experimental values, so for better comparism, experimental data are highly needed.

REFERENCES

1. M. H. Grosjean, M. Zidoune, L. Roue, J. Huot, and R. Schulz, Electrochimica Acta **49**, 2461–2470 (2004).
2. G. Liang and R. Schulz, J. Mater. Sci. **38**, 1179–1184 (2003).
3. Q. M. Peng, K. Li, Z. S. Han, E. D. Wang, Z. G. Xu, R. P. Liu, and Y. J. Tian, J. Biomed. Mater. Res. **101**, 1898 (2013).
4. Y. F. Ding, C. E. Wen, P. Hodgson, and Y. C. Li, J. Mat. Chem. B **2**, 1912–1933 (2014).
5. B. Homayun and A. Afshar, J. Alloy. Compd. **607**, 1–10 (2014).
6. M. S. Daw and M. I. Baskes, Phys. Review Let. **50**, 1285 (1983).
7. R. A. Johnson, Phys. Rev. B **37**, 3924–3931 (1988).
8. R. A. Johnson, Phys. Rev. B **39**, 12554 (1989).
9. R. A. Johnson, Phys. Rev. B **41**, 9717 (1990).
10. R. A. Johnson and D. J. Oh, J. Mat. Res. **4**, 1195–1201 (1989).
11. D. Y. Lin, S. S. Wang, D. L. Peng, M. Li and D. X. Hui, J. Phys.: Condens. Matt. **25**, 105404 (2013).
12. M. I. Baskes and R. A. Johnson, Simul. Mater. Sci. Eng. **2**, 147 (1994).
13. O. O. Popoola, F. Matthew-Ojelabi, G. S. Agunbiade, G. E. Adesakin and T. H. Akande, Int. J. Sci. Res. **6**, 670–673 (2017).
14. B. Zhang and Y. Ouyang, Z. Phys. B **92**, 431–435 (1993).
15. G. S. Agunbiade, F. Matthew-Ojelabi, N. C. Ogbu and T. H. Akande, Int.Org. Sci. Res.: J. Eng. **8**, 75–84 (2018).
16. F. Matthew-Ojelabi, G. S. Agunbiade and T. H. Akande, Int. J. Inn. Res. & Adv. Stud. **4**, 400–404 (2017).
17. T. Akande, F. Matthew-Ojelabi, G. Agunbiade and E. Faweya, Turk. J. Phys. **43**, 606–617 (2019).
18. S. M. Foiles, M. I. Baskes and M. S. Daw, Phys. Rev. B **33**, 7983 (1986).
19. C. Kittel, *Introduction to solid state Physics*, John Wiley and sons. Inc., New York (1996).
20. M. Doyama and J. S. Koehler, Acta Metall. **24**, 871–879 (1976).
21. H. Ledbetter and S. Kim, *Handbook of elastic properties of solids, liquids and gases*, Academic Press, (2001).
22. E. Hashimoto, E. A. Smirnov and T. Kino, J. Phys. F: Met. Phys. **14**, 215 (1984).
23. H. Ogi, S. Kai, H. Ledbetter, R. Tarumi, M. Hirao and K. Takashima, Acta Mater. **52**, 2075–2080 (2004).
24. R. A. Johnson, Phil. Mag. A **63**, 865 (1991).
25. X. Liu, J, B. Adams, F. Ercolessi and J. A. Moriarty, Modelling Simul. Mater. Sci. Eng. **4**, 293 (1996).
26. P. G. Shewmon and F. N. Rhines, Trans. TMS-AIME **200**, 1021 (1954).
27. W. Hu, B. Zhang, B. Huang, F. Gao and D. J. Bacon, J. Phys.: Condens. Matter **13**, 1193–1213 (2001).